Int. J. Multiphase Flow, Vol. 2, pp. 537–548. Pergamon/Elsevier, 1976. Printed in Great Britain.

MEASUREMENT OF DISPERSED TWO-PHASE GAS–LIQUID FLOW BY CROSS CORRELATION OF MODULATED ULTRASONIC SIGNALS

S. T. OLSZOWSKI, J. COULTHARD and R. S. SAYLES

Department of Mechanical Engineering, Teesside Polytechnic, Middlesbrough, Teesside, U.K.

(*Received* 18 *November* 1974)

Abstract—A technique for metering two-phase gas–liquid mixtures is described. The measuring apparatus consists of a concentric constriction device and an ultrasonic cross-correlation velocity meter (Coulthard 1973). The constriction device breaks up the gaseous phase and generates a near-homogeneous type of flow, with characteristics largely independent of those existing in the approach section. The mean velocity of the resulting flow is obtained by cross-correlating the modulations of two parallel ultrasonic beams, transmitted across the pipe. The peak value of the cross-correlation function is found to occur at a time delay virtually equal to the mean transit time of the mixture between the centre lines of the beams.

The main advantages of this type of non-intrusive meter are its averaging capabilities and relative insensitivity to pressure transients.

TWO-PHASE FLOW SYSTEM

The simplest analytical representation of two-phase flow is the homogeneous model (Wallis 1968) in which flow components are treated as a pseudo-homogeneous fluid having average flow properties. Ideally the dispersed mixture is uniform, with the two components moving at equal velocities, with the flow fully developed and one dimensional. This idealisation is hereafter referred to as the ideal homogeneous equilibrium model. Olszowski (1974) investigated some of the difficulties encountered in metering two-phase flow, using standard constriction type devices and concluded that with volumetric gas concentrations up to 30%, it was preferable to meter a finely-dispersed bubble flow generated downstream of an ordinary concentric constriction device. Even in a horizontal conveyor this type of flow existed for some distance downstream of the zone of gross eddying where partial pressure recovery took place, and was the nearest practical approach to the ideal homogeneous equilibrium model.

This investigation showed that pressure waves were generated when two-phase flow was conveyed through certain constrictions. The intensity and time history of such waves, which propagated on both sides of the constriction, was dependent to some degree on the flow pattern in the stream approaching the constriction. These waves affected the measured Bernoulli pressure difference across the metering constriction thus introducing errors in flow measurement by conventional meters. If a 'non-contact' type of flowmeter, whose operation is unaffected by pressure waves, was placed in the region downstream of the disperser, then the measurement accuracy and consistency was improved. The ultrasonic flowmeter satisfied such requirements and was thus chosen to operate in this region.

THE ULTRASONIC FLOWMETER

A diagram of the instrument is shown in figure 1. Two parallel ultrasonic beams spaced a distant L apart are transmitted at right angles to the flow through the walls of the pipe, downstream of the constriction disperser, by piezoelectric transducers T_1 and T_2 to be received by similar transducers R_1 and R_2 situated diametrically opposite. The ultrasonic beams are modulated by acoustic impedance changes within the moving fluid, and the modulation envelopes are used as signals $x(t)$ and $y(t)$ to be correlated. The separation of the beams L is such that the modulation mechanism at A does not lose its identity on reaching B. The peak value of the cross-correlation function $\psi_{xy}(\tau)$ occurs at a value of $\tau = \tau_m$ where

$$\tau_m = L/U. \qquad [1]$$

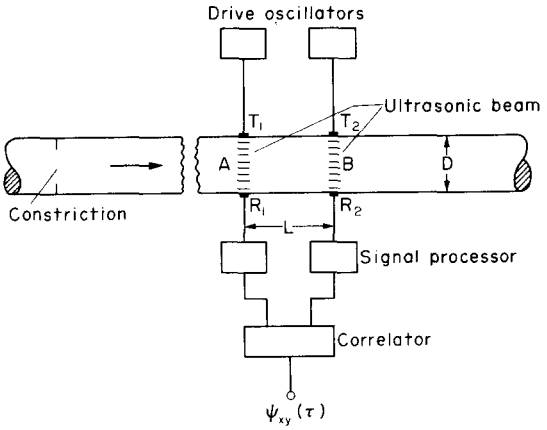

Figure 1. Flow measuring principle.

U is the mean flow velocity and $\psi_{xy}(\tau)$ is given by the relation

$$\psi_{xy}(\tau) = \lim_{T\to\infty} \frac{1}{T} \int_0^T x(t)y(t+\tau)\,dt. \qquad [2]$$

The transducer assembly is assumed to be situated in a coordinate system similar to the one adopted by Fisher & Krause (1967) shown in figure 2. In single-phase fluids modulation of the acoustic wave is mainly due to absorption and refraction caused by turbulent pressure fluctuations, but in two-phase gas–liquid mixtures specular acoustic reflection occurs from the gas bubbles and this produces the dominant modulation component.

Consider a circular transducer of radius 'a' transmitting a parallel beam of acoustic energy across the tube of diameter D. If the acoustic intensity of the ultrasonic wave can be assumed to decrease exponentially with distance from the transmitter, then the amplitude of the signal recorded at receiver A is:

$$I_1(t) = I_0 \exp\left\{-\int_V K(\xi, \eta, \zeta, t)\,dV\right\}. \qquad [3]$$

dV is a volume element of the acoustic field of volume V, I_0 is the acoustic intensity at the transmitter and K is an attenuation coefficient at time t and position (ξ, η, ζ), accounting for all possible sources of acoustic attenuation.

K can be written as the sum of its time-averaged mean value $\langle K(\xi, \eta, \zeta)\rangle$ together with a fluctuation about this value $k(\xi, \eta, \zeta, t)$ then

$$I_1(t) = I_0 \exp\left\{-\int_V \langle K(\xi, \eta, \zeta)\rangle\,dV\right\} \exp\left\{-\int_V k(\xi, \eta, \zeta, t)\,dV\right\}. \qquad [4]$$

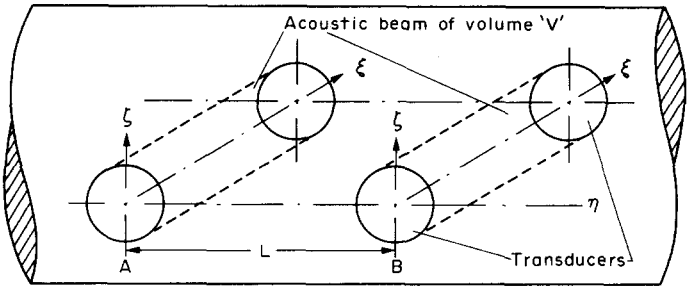

Figure 2. Co-ordinate system.

If $k(\xi, \eta, \zeta, t) \ll \langle K(\xi, \eta, \zeta) \rangle$ then the exponent can be linearised:

$$\exp\left\{-\int_V k(\xi, \eta, \zeta, t)\,\mathrm{d}V\right\} \doteq 1 - \int_V k(\xi, \eta, \zeta, t)\,\mathrm{d}V,$$

and [4] becomes:

$$I_1(t) = I_0 \exp\left\{-\int_V \langle K(\xi, \eta, \zeta)\rangle\,\mathrm{d}V\right\}\left\{1 - \int_V k(\xi, \eta, \zeta, t)\,\mathrm{d}V\right\}. \qquad [4a]$$

Let the time-averaged mean value of $I_1(t)$ be $\langle I_1 \rangle$
where

$$\langle I_1 \rangle = I_0 \exp\left\{-\int_V \langle K(\xi, \eta, \zeta)\rangle\,\mathrm{d}V\right\}.$$

Equation [4a] thus becomes:

$$I_1(t) = \langle I_1 \rangle - \langle I_1 \rangle \int_V k(\xi, \eta, \zeta, t)\,\mathrm{d}V. \qquad [5]$$

The time-varying component of the signal is given by the expression:

$$x(t) = -\langle I_1 \rangle \int_V k(\xi, \eta, \zeta, t)\,\mathrm{d}V. \qquad [6]$$

Demodulation of the received signal removes $\langle I_1 \rangle$ so that the space–time correlations of the signals $x(t)$ and $y(t)$ yield:

$$\psi_{xy}(L, \tau) = \lim_{T\to\infty} \frac{1}{T} \int_0^T \left\{\int_{V_1} k(\xi, \eta, \zeta, t)\,\mathrm{d}V_1 \times \int_{V_2} k(\xi, \eta + L, \zeta, t + \tau)\,\mathrm{d}V_2\right\} \mathrm{d}t, \qquad [7]$$

where V_1 and V_2 are the volumes of acoustic fields A and B.

If the transducer diameter and its ratio to the conveyor diameter C_A is small (say less than 0.1) then the convection velocity can be assumed constant within any section of the acoustic beam. Therefore $k(\xi, \eta, \zeta, t) = k(\xi, t)$ so that the demodulated form of [6] is

$$x(t) = -\int_V k(\xi, t)\,\mathrm{d}V \qquad [6a]$$

which for a circular transducer of radius a is

$$x(t) = \pi a^2 \int_0^D k(\xi, t)\,\mathrm{d}\xi.$$

For the instrument used in in the experiments described $C_A = 0.2$ so that some variations in convection velocity occurs in sections of the acoustic beam close to the transmitting and receiving transducers.

In two-phase flow, reflections from the dispersed gas phase and from the curved surfaces of the pipe cause some acoustic energy to arrive at the receiver from all points within a cylindrical

volume having a diameter equal to that of the pipe and a length equal to the diameter of the transducer. Flow data is thus more closely related to an area integral across the pipe cross-section. Figure 3 shows photographs of typical receiver and processed signals obtained from single and two-phase flow measurements. The difference in depths of modulation are clearly apparent.

TEST RIG AND EXPERIMENTAL METHOD

A diagram of the test rig is shown in figure 4. Water was recirculated by means of a variable-speed centrifugal pump. Dry compressed air could be introduced into the line through a multi-orifice type injector immediately down-stream of a pipe bend to enhance mixing. The air was released in the weir-gauging tank and the time taken for water to pass across the tank was sufficiently long to prevent carry-over of air in suspension. To avoid absorption of the injected air during the two-phase flow measurements, the water was saturated with air prior to testing. Mass-flow rates of both components were measured before mixing by means of calibrated meters.

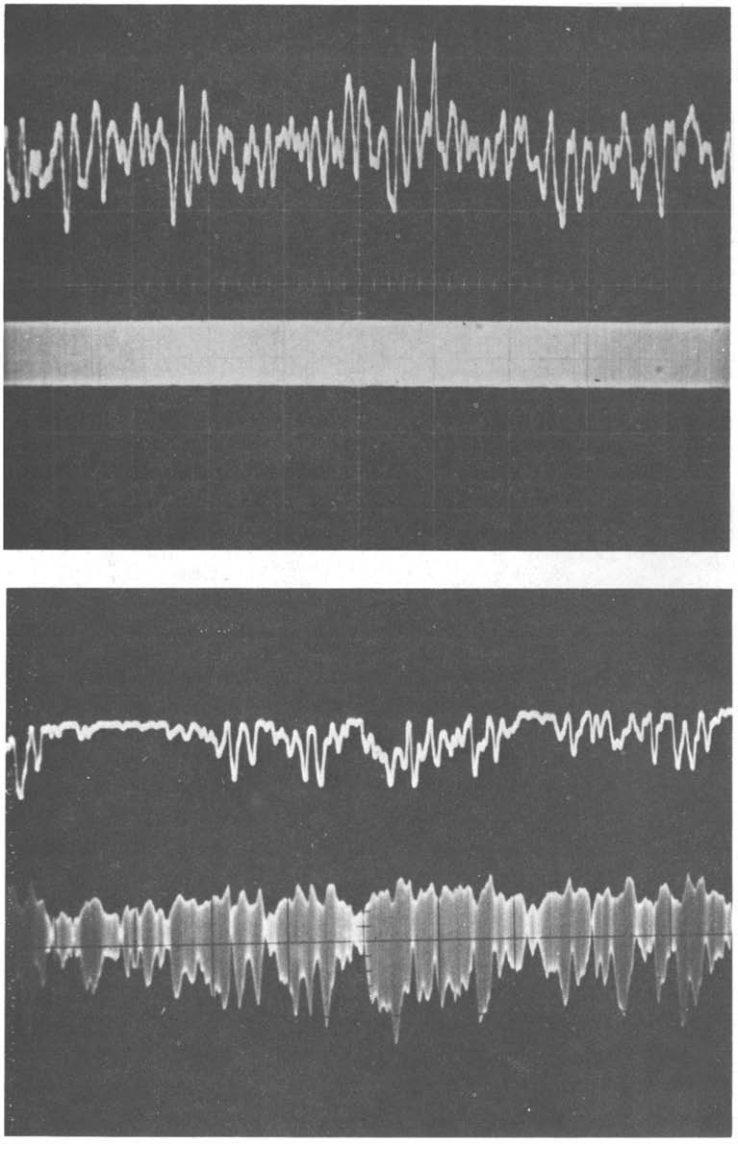

Figure 3. Two-phase liquid–gas flow. Upper trace—correlated signal; lower trace—received signal. Upper plate—single-phase flow. Lower plate—two-phase flow.

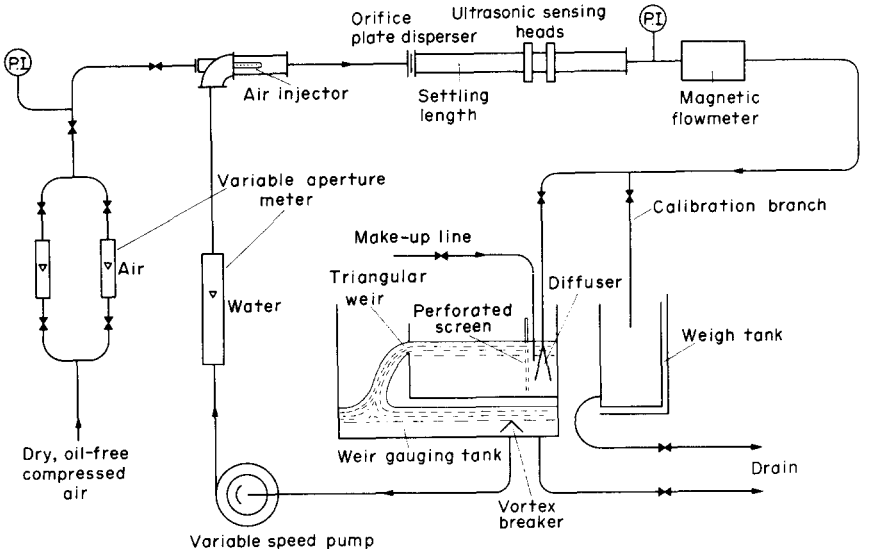

Figure 4. Line diagram of test rig.

The working section of the ultrasonic meter was a translucent pipe of 50.8 mm bore and the disperser chosen was a sharp-edged concentric orifice plate of area ratio 0.5 situated 15 diameters upstream of the first set of ultrasonic transducers. Each transducer assembly consisted of two flat circular piezoelectric discs having a nominal resonant frequency of 2 MHz attached diametrically opposite each other to movable aluminium rings. These assemblies were situated one pipe diameter apart. A schematic diagram of the electronic processing circuits used is given in figures 5 and 6. The schematic diagram describes an ideal processor suitable for monitoring wide ranges of single and two-phase flow. AGC in the high-frequency circuit ensures that the voltage presented to the detector remains at an optimum value. Rectification of the modulation signal is used to control the gain of the low-frequency amplifier so that the circuits can handle wide variations in depths of modulation. In the experiments described the gain of the low frequency amplifier was manually controlled. Tuning of the high-frequency amplifier is necessary to eliminate signals due to pipe vibration.

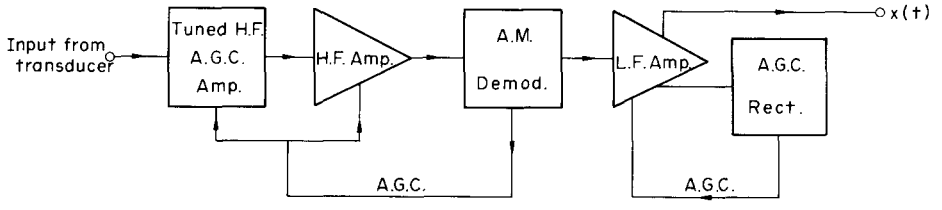

Figure 5. Schematic diagram of the signal processor.

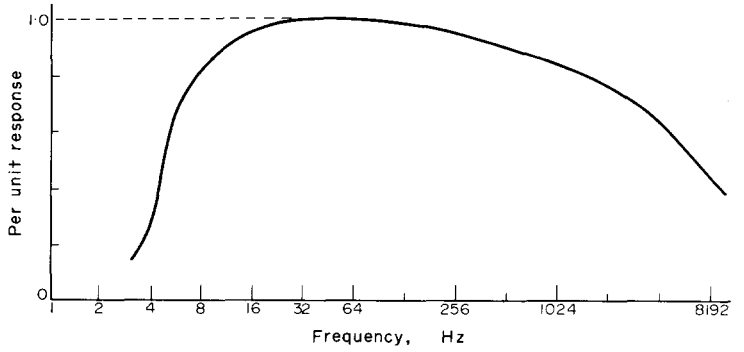

Figure 6. Frequency response of ultrasonic flowmeter.

A magnetic flowmeter detector head was installed immediately downstream of the ultrasonic meter section. The purpose of the magnetic flowmeter was to provide quantitative verification of the near-zero relative velocity between the two components due to the action of the concentric disperser.

For each constant air flow, the flow of water was varied from the maximum possible value to some minimum below which the action of the disperser proved inadequate to break up large elongated air plugs at the threshold of slug type of flow. Under these conditions severe pressure waves emanating from the disperser due to slugging effects produced the predominant modulation signal component and the cross-correlation curve consisted of a large peak due to the propagation velocity of shock waves which tended to mask and peak due to the flow velocity. This is illustrated in figure 7.

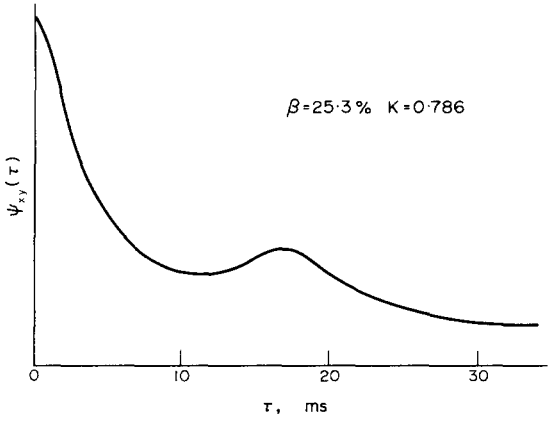

Figure 7. Cross-correlation curve obtained in the presence of intense shock waves.

The flow pattern upstream of the disperser varied from 'bubble' type through 'plug' type to separated flow when frothy slugs began to be conveyed at a much greater velocity than average liquid velocity. The dispersive action was effective and the ultrasonic meter functioned satisfactorily even when agglomerations of air bubbles of varying sizes were conveyed intermittently following the breaking up of plugs, until the final slugging stage was reached. Figures 8 and 9 are photographs of typical flow patterns immediately downstream of the constriction. Figure 9 clearly shows intermittent action due to the breaking up of large plugs of air.

EVALUATION OF RESULTS

1. *Properties of the correlated signals*

The peak value of $\psi_{xy}(\tau)$ was taken as the mean transit time of the fluid between the centre lines of the ultrasonic beams A and B in figure 1 and this was compared with measured results. Recent investigations by Davies & Mercer (1973) and the earlier work of Stegan & Van Atta (1970) and Fisher & Davies (1969) showed how temporal velocity fluctuations appear as phase variations which are not proportional to frequency. This is caused by some frequency components having different transit times between the monitoring points. The effect is to produce cross-correlation functions which are skewed and can introduce significant errors. It was therefore necessary to examine whether such effects were significant.

For the non-frozen flow pattern the non-proportional relationship means that the phase velocity U is no longer constant as in the frozen case but is a function of frequency.

$$U = U(f). \qquad [8]$$

The phase-frequency relationship is given by the relation

$$\theta_i = 2\pi f_i \tau_i, \qquad [9]$$

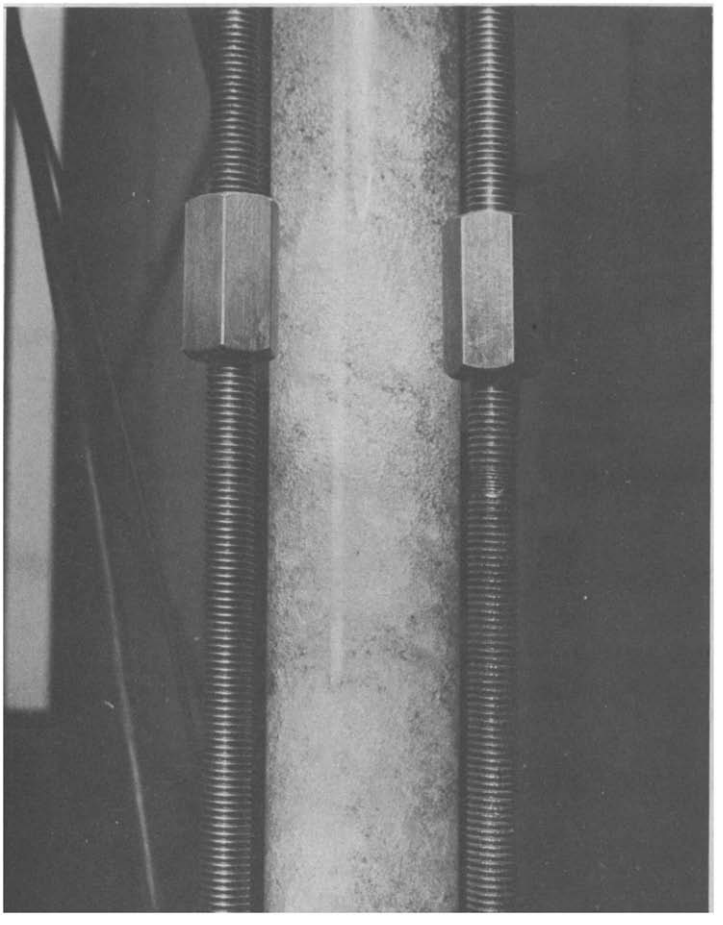

Figure 8. Bubble flow immediately downstream of the disperser. Air volume ratio β = 10%.

where τ_i is the time-of-flight of the frequency component f_i. Let L be the spacing between metering points, then

$$U_i = \frac{2\pi f_i L}{\theta_i}. \qquad [10]$$

To obtain the best estimate of U corresponding to all frequency components, the normalised modulus spectrum can be used as a weighting factor:

$$W(f) = \frac{G_{xy}(f_i)}{G_{xy}(f_0)}. \qquad [11]$$

The mean weighted velocity is therefore given by

$$U = \frac{2\pi L \sum_{i=0}^{i=N} W(f_i) \dfrac{f_i}{\theta(f_i)}}{\sum_{i=0}^{i=N} W(f_i)}, \qquad [12]$$

where N is the number of discrete spectral estimates. Figure 10 gives a typical measured normalised modulus or weighting function plotted against frequency. This shows that the effect of [12] is to bias U towards the lower frequency components where the power in the spectrum is high. Also deviations from phase-frequency proportionality which are responsible for skewness

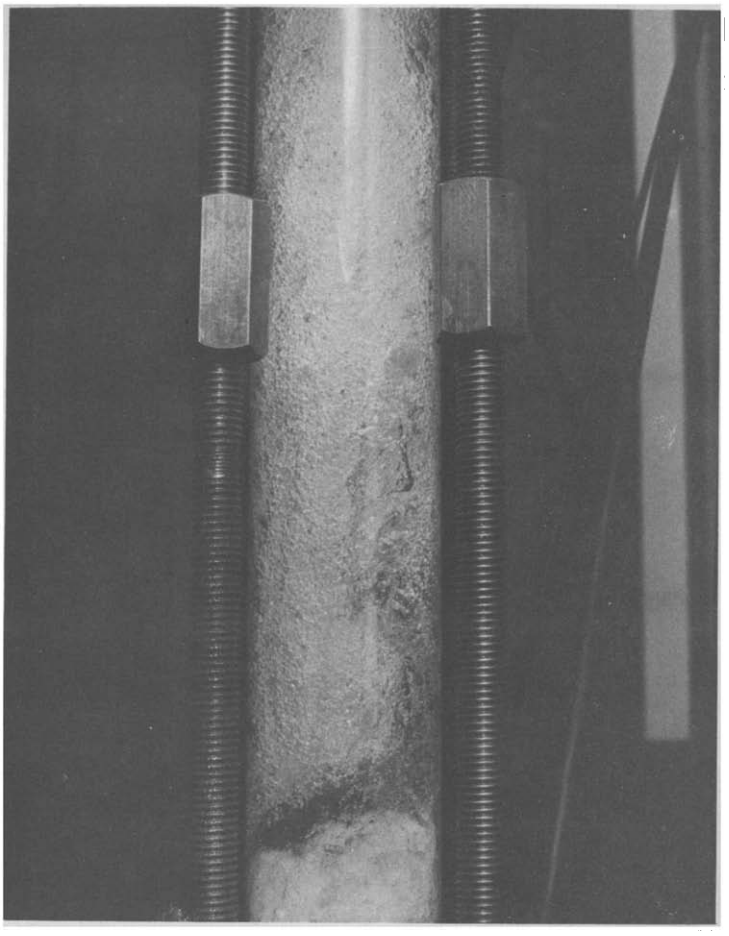

Figure 9. Bubble flow immediately downstream of the disperser. Air volume $\beta = 30\%$.

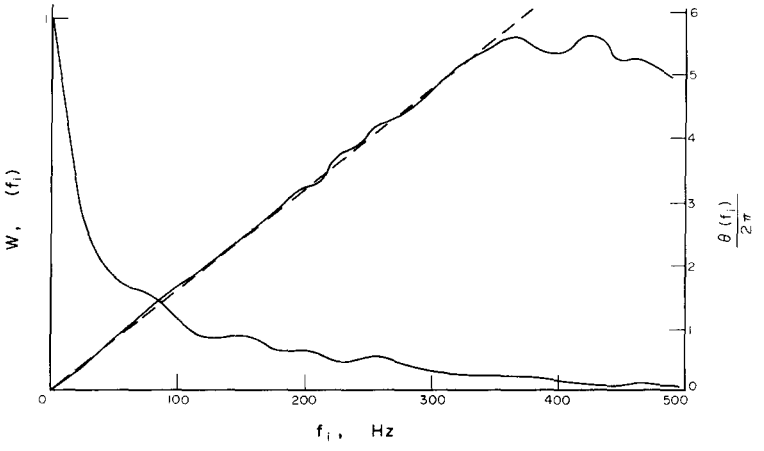

Figure 10. Weighting function $W(f_i)$ and phase $(f_i)/2\pi$ vs frequency (f_i). The dashed line represents the ideal or frozen flow pattern.

of the cross-correlation curve occur at high frequencies and are accompanied by low values of weighting function and are therefore insignificant.

Figure 11 shows typical cross-correlation functions and corresponding cross-spectra, the latter plotted on polar coordinates. The symmetry of the correlogram emphasises the almost straight-line relationship between phase and frequency of the cross-power spectrum. Figure 12

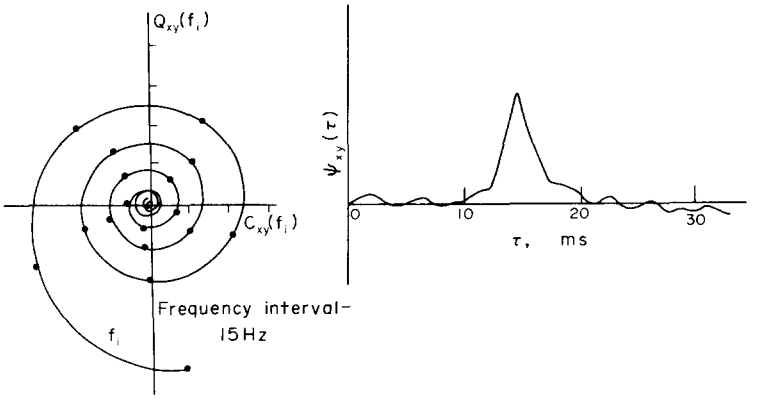

Figure 11. Cross-correlation curve and cross-power spectrum without shock wave.

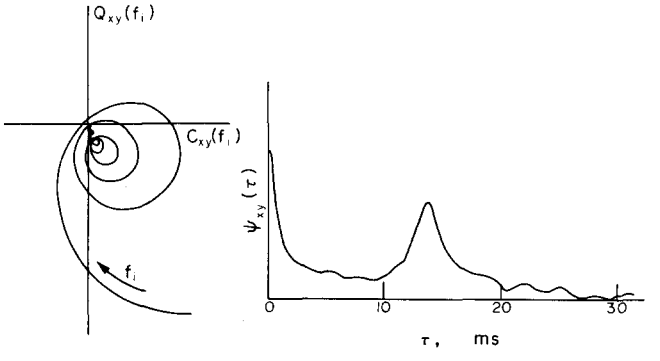

Figure 12. Cross-correlation curve and cross-power spectrum with shock wave. Cross-correlation function ($\psi_{xy}(\tau)$), $V^2x\ 10^{-2}$, vs time delay (τ)ms, and corresponding polar spectra. (Frequency interval is 15 Hz.)

shows that the spectrum contour becomes asymmetric about the origin when the amplitude of a pressure wave component increases relative to the convection peak. These results show that in all cases it is valid to assume that the peak value of $\psi_{xy}(\tau)$ occurs at a time delay giving a reasonable estimate of mean flow velocity.

2. *Flow parameters and measurements*

The measured mass flow rates of the two components were converted into volume flow rates at the ultrasonic meter section. To conform with the ideal homogeneous equilibrium flow assumption, the component flow rates were compounded algebraically to obtain the mean velocity of the mixture. This was compared with the velocity deduced from the transit time inferred from the cross-correlation peak.

The magnetic flowmeter output was assumed to measure the velocity of the water component and from the estimated remaining flow area, the velocity of the air component was deduced.

In presenting the results the following two-phase gas–liquid flow parameters are used:

Mass dryness fraction (mixture quality) $X = (G_G/G_T)$ where $G_T = G_G + G_L$.

Ratio of gas flow rate by volume to that of mixture,

$$\beta = \frac{Q_G}{Q_T},$$

where

$$Q_T = Q_G + Q_L,$$

Also,

$$G_G = \rho_G Q_G \quad \text{and} \quad G_L = \rho_L Q_L.$$

Velocity ratio,

$$K = \frac{U_G}{U_L}.$$

Void fraction (proportion of cross-section occupied by gas), $\alpha = (A_G/A)$, where $A = A_L + A_G$.

For an ideal homogeneous equilibrium model, the void draction α and the gas volume ratio β are the same, and the velocity ratio K is unity. Hence

$$U_{HOM} = \frac{Q_T}{A},$$

$$\rho_{HOM} = \frac{G_T}{AU_{HOM}} = \rho_G + (1-\alpha)\rho_L,$$

and

$$\frac{1}{\rho_{HOM}} = \frac{x}{\rho_G} + \frac{1-x}{\rho_L}.$$

Solving for x,

$$x = \frac{AU_{HOM}\rho_G\rho_L}{G_T(\rho_L - \rho_G)} - \frac{\rho_G}{\rho_L - \rho_G}. \qquad [13]$$

If the term $\rho_G/(\rho_L - \rho_G)$ is small, compared to the first term in [13] then

$$x = \frac{AU_{HOM}\rho_G\rho_L}{G_T(\rho_L - \rho_G)}.$$

In the above notation: A, flow cross-section; U, velocity; ρ, mass density.

Subscripts: G, relates to gas (i.e. air in this case); L, relates to liquid (i.e. water in this case); HOM, relates to the ideal homogeneous equilibrium, flow model; T, designates the total flow.

DISCUSSION OF RESULTS

The tests were confined to low-quality low-pressure air–water mixtures with the ultrasonic velocity meter situated downstream of a simple disperser in the form of a concentric thin sharp-edged orifice plate. The range of test conditions were as follows:

Mass velocity range 52×10^5–133×10^5 kg/m^{2}hr.

Mixture velocity range 1.6–4.1 m/sec.

Quality range $x = 0.13 \times 10^{-4}$ to 12.3×10^{-4}.

Gas volume ratio range $\beta = 0.6$ to 43.6%.

Static pressure range 1.1 to 2.1 bar abs.

In the tests conducted, the pattern of flow varied from that of minute air globules seemingly uniformly dispersed in a liquid matrix (the mixture having a 'milky' appearance), to that comprising discontinuous agglomerations of varying-sized air bubbles. Under the latter limiting condition, the motion was 'pseudo-cyclic' following the dispersion of intermittently occurring air plugs. Pressure waves generated by this action were propagated in the direction of flow and these imparted an oscillatory component of motion to the mixture. The tests were terminated when severe pressure waves generated by the disperser obscured the correlation measurements. Those conditions corresponded with an essentially separated flow upstream of the disperser, aggravated by the occurrence of frothy slugs.

The information deduced from the magnetic flowmeter verified the assumption of unity velocity ratio, with a ±10% scatter, under conditions of uniform and continuous dispersion of non-conducting 'pores' in the liquid matrix. The scatter was attributed to experimental errors arising from small differences in cross-sectional areas (between that of the detector and those attributed to the liquid component). At higher values of the gas–volume ratio, especially under conditions of intermittent formation of clouds of varying sized air bubbles, this 'inference' method yielded results which were unacceptable on physical grounds.

In figures 13 and 14 mean mixture velocity as measured by the ultrasonic flowmeter are

plotted versus mixture velocity based upon the assumed ideal homogeneous equilibrium model. Lines of equi-percentage differences are superimposed to aid interpretation. Figure 13 contrasts the results of two-phase air–water flow at low gas volume ratio ($\beta < 10\%$) with those of mono-phase water flow. These results confirm the essential difference in the mechanism of modulation of the ultrasonic beams when transmitted across a homogeneous mono-phase stream on the one hand and across a thoroughly dispersed two phase mixture on the other.

Figure 14 gives the results of dispersed two-phase flow for the whole spectrum of the gas volume ratios used. The velocities of two-phase mixtures at low gas–volume ratios ($\beta < 10\%$), measured by the ultrasonic meter, closely correspond with those based on component flow measurements processed to conform with the assumed ideal homogeneous equilibrium model. As

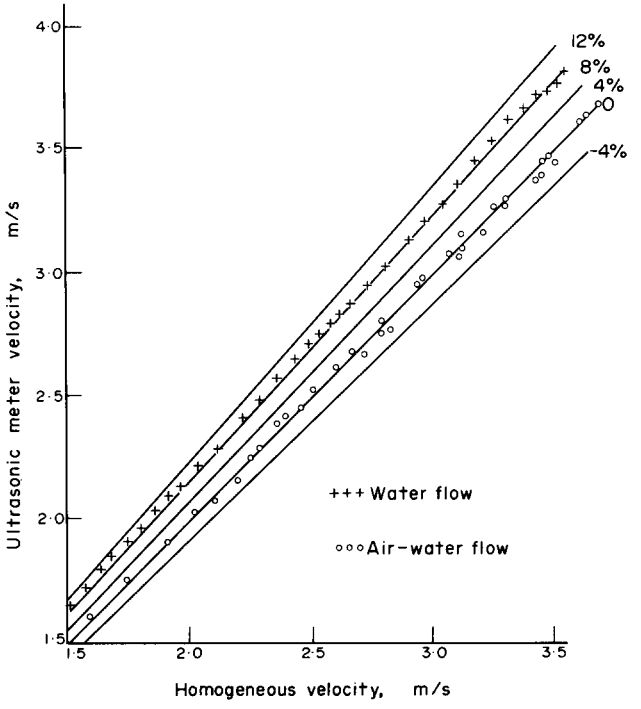

Figure 13. Performance of ultrasonic meter on water flow and air–water flow at low air volume fractions.

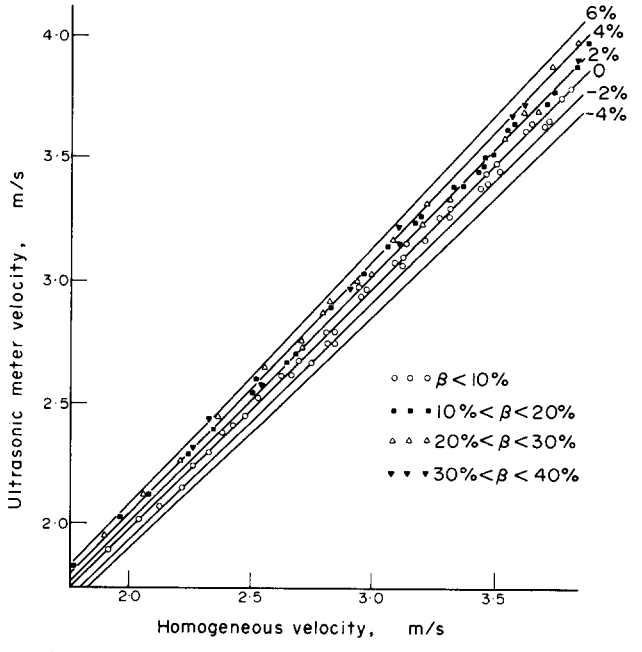

Figure 14. Performance of ultrasonic meter on air–water flow at varying air volume fractions.

the gas-bubble population increases and the morphological arrangement of the two phases becomes less orderly, the velocities indicated by the ultrasonic meter progressively exceed the homogeneous velocities by a maximum of about 4% with this type of disperser. This is presumably due to the velocity of the air bubbles exceeding that of the water i.e. $K > 1$.

With both the monophase and two-phase flows at 'constant' void fractions, the error of the ultrasonic meter increases as the velocity decreases—by approximately 2% in the range of velocities tested. One possible explanation is the loss of information from some spectral components due to the decay of correlation over the fixed distance between the beams. This would be one of the causes of the departure from direct proportionality in the phase-frequency relationship mentioned earlier.

CONCLUSIONS

This paper shows that if an attempt is made to produce a pseudo-homogeneous dispersed flow, such as that created downstream of a simple concentric constriction, then conditions exist which facilitate measurement by correlation methods. The measured cross-correlation functions and their Fourier transforms indicate that in this application dispersed two-phase fluid retains an almost 'frozen' flow pattern for at least one pipe diameter in the region where a homogeneous two-phase fluid is assumed to exist.

It is reasonable to assume that the techniques described apply to other gas–liquid or vapour–liquid mixtures providing that an adequate disperser is chosen and pressure waves on the ultrasonic meter are minimized. The pressure waves, at their worst, tend to mask (not to falsify) the peak of the cross-correlation function.

Although the derived signals contain no information concerning the mass flow or mixture quality, the experiments indicate that the velocity measurement can be determined accurately with reference to the simple mathematical model of two-phase flow. Working in conjunction with a calibrated transducer to sense the mixture intensity, the ultrasonic correlation meter yields information from which the total mass flow can be obtained.

The ultrasonic correlation meter can also be used as a quality meter in a system, involving a two-phase single-component mixture. Working in conjunction with an all-liquid or all-vapour flowmeter which measures the total mass flow, the ultrasonic meter situated downstream of an efficient disperser indicates the homogeneous velocity. From the knowledge of thermal conditions at the ultrasonic meter working section, the phase densities can be ascertained. Hence the mixture quality can be determined using[13] or its degenerated form, when justified. If the thermodynamic properties of the mixture at the working section remain invariant, the mixture quality vary inversely as the product of the total mass flow rate and the transit time between the ultrasonic beams.

REFERENCES

COULTHARD, J. 1973 Ultrasonic cross correlation flowmeters. *Ultrasonics* **2**, 83–88.

DAVIES, P. O. A. L. & MERCER, C. A. 1973 Phase Velocity Measurements Using the Cross Power Spectrum. I.M.C. International Symposium on Measurement and Process Identification by Correlation and Spectral Techniques.

FISHER, M. J. & DAVIES, P. O. A. L. 1964 Correlation measurements in a non-frozen pattern of turbulence. *J. Fluid Mech.* **18**, 97–116.

FISHER, M. J. & KRAUSE, F. R. 1967 The crossed beam correlation technique. *J. Fluid Mech.* **28**, 705–717.

OLSZOWSKI, S. T. 1974 The onset of instability, pressure transients and flow oscillations in two-phase two-component flow metering. C.N.A.A. M. Phil. Thesis, Teeside Polytechnic.

STEGAN, G. R. & VAN ATTA, C. W. 1970 A technique for phase speed measurements in turbulent flow. *J. Fluid Mech.* **42**, 689–699.

WALLIS, G. B. 1968 *One Dimensional Two-Phase Flow.* McGraw-Hill.